

Characterization of TDP-4-Keto-6-deoxy-D-glucose-3,4-ketoisomerase from the D-Mycaminose Biosynthetic Pathway of *Streptomyces fradiae*: In Vitro Activity and Substrate Specificity Studies[†]

Charles E. Melançon, III,[‡] Lin Hong,^{‡,||} Jess A. White,[§] Yung-nan Liu,^{||} and Hung-wen Liu^{*,‡,§,||}

Division of Medicinal Chemistry, College of Pharmacy, Department of Chemistry and Biochemistry, and Institute for Cellular and Molecular Biology, University of Texas, Austin, Texas 78712

Received September 13, 2006; Revised Manuscript Received November 14, 2006

ABSTRACT: Deoxysugars are critical structural elements for the bioactivity of many natural products. Ongoing work on elucidating a variety of deoxysugar biosynthetic pathways has paved the way for manipulation of these pathways for the generation of structurally diverse glycosylated natural products. In the course of this work, the biosynthesis of D-mycaminose in the tylosin pathway of *Streptomyces fradiae* was investigated. Attempts to reconstitute the entire mycaminose biosynthetic machinery in a heterologous host led to the discovery of a previously overlooked gene, *tyl1a*, encoding an enzyme thought to convert TDP-4-keto-6-deoxy-D-glucose to TDP-3-keto-6-deoxy-D-glucose, a 3,4-ketoisomerization reaction in the pathway. Tyl1a has now been overexpressed, purified, and assayed, and its activity has been verified by product analysis. Incubation of Tyl1a and the C-3 aminotransferase TylB, the next enzyme in the pathway, produced TDP-3-amino-3,6-dideoxy-D-glucose, confirming that these two enzymes act sequentially. Steady state kinetic parameters of the Tyl1a-catalyzed reaction were determined, and the ability of Tyl1a and TylB to process a C-2 deoxygenated substrate and a CDP-linked substrate was also demonstrated. Enzymes catalyzing 3,4-ketoisomerization of hexoses represent a new class of enzymes involved in unusual sugar biosynthesis. The fact that Tyl1a exhibits a relaxed substrate specificity holds potential for future deoxysugar biosynthetic engineering endeavors.

Deoxysugars, such as D-mycaminose (**1**, Scheme 1), are present in the structures of many secondary metabolites possessing antigenic, antibiotic, and chemotherapeutic properties (*1*). These unusual sugars have been shown to be important for the biological activities of the parent compounds in functional studies of natural products with altered glycosylation patterns (*2, 3*) and in structural studies of glycosylated natural products complexed with their targets (*4*). Due to the direct role of deoxysugars in conferring natural product bioactivity, there has been much interest in elucidating deoxysugar biosynthetic pathways (*5–10*). Recently, the feasibility of manipulating the sugar biosynthetic machinery to generate new glycosylated natural products has been demonstrated (*6, 8, 11–13*). However, to further exploit this strategy, enzymes involved in the formation of a diverse set of deoxysugars must be identified, their activities demonstrated, preferred substrates identified, and tolerance for other substrates assessed. A detailed understanding of the biochemical properties of these enzymes is important because any rational attempt to effectively utilize a specific enzyme in biosynthetic applications requires an understanding of the details of its catalytic process.

The biosynthesis of mycaminose (**1**) has been studied for more than 10 years. This 3-*N,N*-dimethylamino-3,6-dideoxy-hexose is found as a substituent on a number of 16-membered ring macrolide antibiotics, including leucomycins, carbomycins, maridomycins, platenomycins, midcamycins, and spiramycins (*14*). It is also the first sugar attached to tylactone (**2**), a 16-member macrolactone, in the formation of tylosin (**3**) in *Streptomyces fradiae* (Scheme 1). Extensive genetic and phenotypic complementation studies revealed the genetic organization of the tylosin (*tyl*) biosynthetic gene cluster in which the *tylG* region harbors the polyketide synthase (PKS)¹ genes for making tylactone, and the flanking *tylLM*, *tylIBA*, and *tylCK* regions contain the genes for unusual sugar formation (*15*). The *tylLM*, *tylIBA*, and *tylCK* regions were

[†] This work was supported in part by National Institutes of Health Grants GM35906 and GM54346.

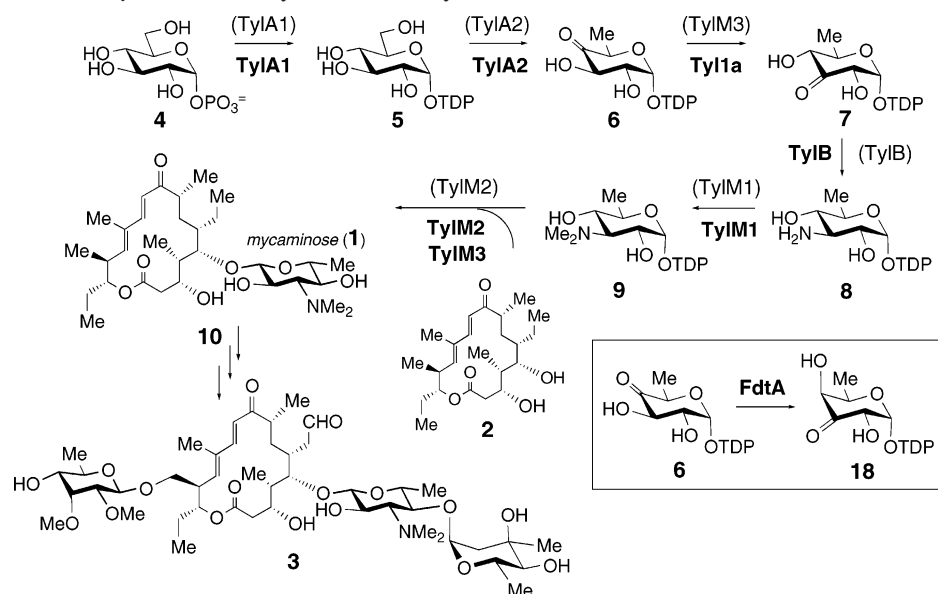
* To whom correspondence should be addressed. Phone: (512) 232-7811. Fax: (512) 471-2746. E-mail: h.w.liu@mail.utexas.edu.

[‡] Department of Chemistry and Biochemistry.

[§] Institute for Cellular and Molecular Biology.

^{||} Division of Medicinal Chemistry, College of Pharmacy.

¹ Abbreviations: CDP, cytidine 5'-diphosphate; CI-MS, chemical ionization mass spectrometry; CTP, cytidine 5'-triphosphate; DMSO, dimethyl sulfoxide; EDTA, ethylenediaminetetraacetic acid; ESI-MS, electrospray ionization mass spectrometry; FPLC, fast protein liquid chromatography; GDP, guanine 5'-diphosphate; HPLC, high-performance liquid chromatography; IPTG, isopropyl β -D-thiogalactoside; LB, Luria-Bertani; NCBI, National Center for Biotechnology Information; NDP, nucleotide 5'-diphosphate; NMR, nuclear magnetic resonance; ORF, open reading frame; PAGE, polyacrylamide gel electrophoresis; PCR, polymerase chain reaction; PEP, phosphoenolpyruvate; PKS, polyketide synthase; PLP, pyridoxal 5'-phosphate; PMSF, phenylmethanesulfonyl fluoride; SAM, S-adenosylmethionine; SDS, sodium dodecyl sulfate; TDP, thymidine 5'-diphosphate; TPCK, N-p-tosyl-L-phenylalanine; TTP, thymidine 5'-triphosphate; Tyl1a, TDP-4-keto-6-deoxy-D-glucose 3,4-ketoisomerase; TylB, TDP-3-keto-6-deoxy-D-glucose 3-aminotransferase; UDP, uridine 5'-diphosphate; UTP, uridine 5'-triphosphate.



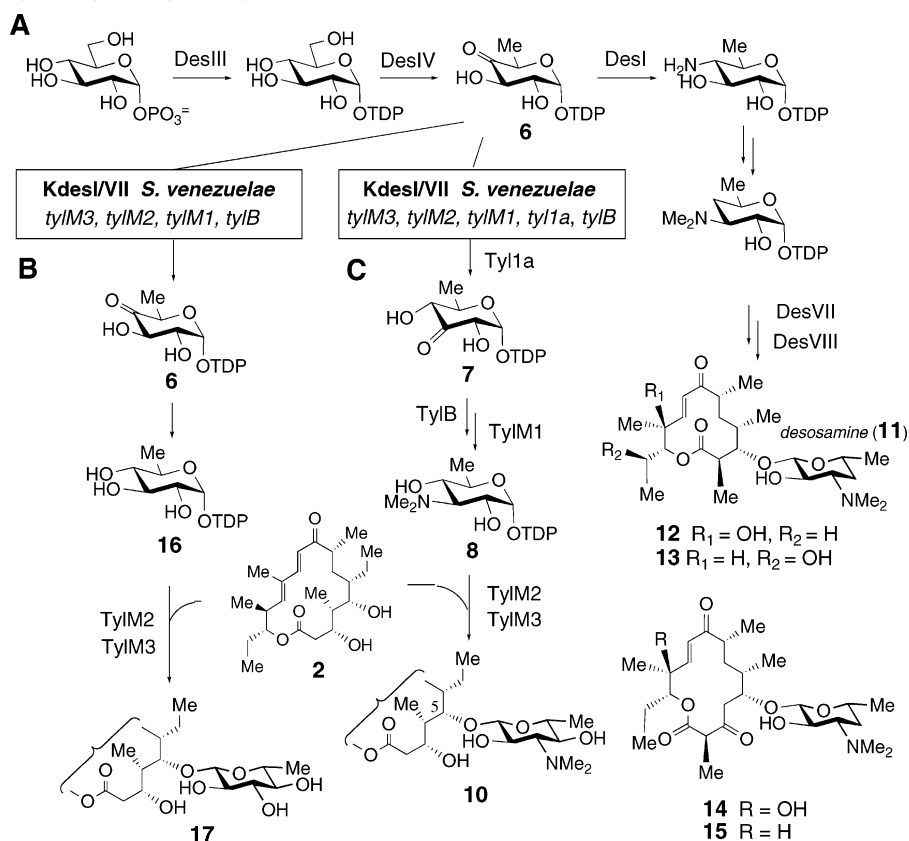
sequenced in previous studies, and 17 open reading frames (ORFs) were identified within these regions (16). Sequence similarities with other sugar biosynthetic genes, especially those reported by Cundliffe and co-workers who had also sequenced the *tylIBA* and *tylLM* regions of the *tyl* cluster (17), led to the assignment of *tylA1*, *tylA2*, *tylB*, *tylM1*, *tylM2*, and *tylM3* as genes involved in mycaminose formation and attachment.

While most of the steps in the proposed mycaminose biosynthetic pathway are supported by sequence alignment data or biochemical evidence, the process by which TDP-4-keto-6-deoxy-D-glucose (**6**) isomerizes to **7** remains unknown. On the basis of two early reports in which a portion of **6** was transformed to **7** during purification by Dowex-1 ion exchange chromatography, a reversible nonenzymatic ketoisomerization between **6** and **7** was thought to occur (19, 20). However, in our study of TylB, when the reaction was run in reverse using **8** and α -ketoglutarate as substrates, only **7** was produced and no trace of **6** was detected. Also, no product was formed upon incubation of **6** with TylB. These results indicated that, at least under the in vitro conditions that were used, there was no chemical isomerization between

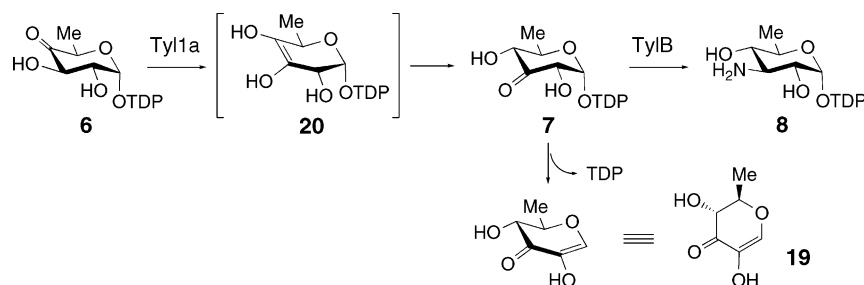
Subsequent attempts to reconstitute the mycaminosose biosynthetic pathway in a nonproducing strain showed that expression of *tylB*, *tylM1*, *tylM2*, and *tylM3* failed to convert **6** to TDP-D-mycaminose (**9**) and couple **9** to ty lactone (**2**). These studies were performed by heterologous expression of *tylB*, *tylM1*, *tylM2*, and *tylM3* in a mutant (KdesI/VII) of *Streptomyces venezuelae*, which is the producer of the D-desosamine (**11**)-containing macrolide antibiotics methymycin (**12**), neomethymycin (**13**), pikromycin (**14**), and narbomycin (**15**) (Scheme 2A). With the *desI* and *desVII* genes disrupted, intermediate **6** was expected to accumulate in vivo. We also expected that expression of *tylB*, *tylM1*, *tylM2*, and *tylM3* would produce all the necessary enzymes to convert **6** to TDP-D-mycaminose (**9**), which could then be used by TylM2 to glycosylate appropriate aglycones. Surprisingly, feeding exogenous ty lactone (**2**) to this recombinant strain led to quinovosyl ty lactone (**17**) rather than the anticipated mycaminosyl ty lactone (**10**, Scheme 2B) (**8**). Production of quinovosylated macrolides had previously been observed in an *S. venezuelae* mutant in which *desI* was disrupted. It was proposed that quinovose was generated by C-4 reduction of **6** by a nonspecific reductase to give **16** in the KdesI mutant (**21**). A similar reduction of **6** to **16** likely occurs in the KdesI/VII mutant. Thus, the results given above strongly suggested that conversion of **6** to **7** did not occur in the recombinant strain.

The inability to reconstitute the mycaminose pathway with the *tylB*, *tylM1*, *tylM2*, and *tylM3* genes in the experiment described above prompted us to re-examine all unassigned open reading frames (ORFs) in the tylosin gene cluster. This effort led to the identification of an ORF, *la*, which is immediately downstream from and translationally coupled

Scheme 2: (A) Biosynthesis of Desosamine (**11**) and Its Incorporation into Methymycin (**12**), Neomethymycin (**13**), Pikromycin (**14**), and Narbomycin (**15**) in *S. venezuelae*, (B) Pathway for the Formation of Quinovosyltylactone (**17**) in the KdesI/KdesVII/*tylM3*, *tylM2*, *tylM1*, *tylB* Mutant, and (C) Pathway for the Formation of Mycaminosyltylactone (**10**) in the KdesI/KdesVII/*tyl1a*, *tylM3*, *tylM2*, *tylM1*, *tylB* Mutant



Scheme 3: Conversion of **6** to **8** by TyI1a and TyIB as Part of the Biosynthesis of TDP-D-Mycaminose^a

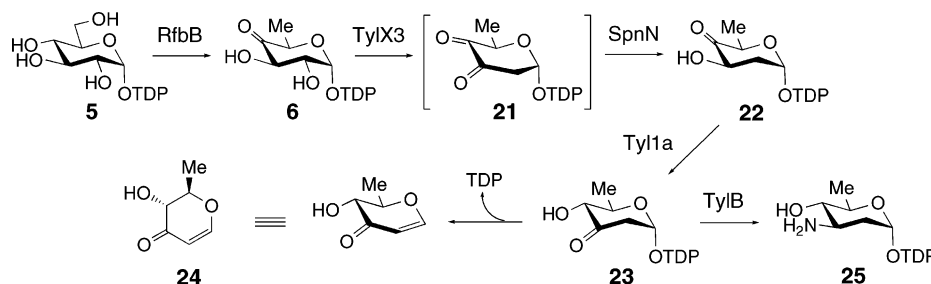


^a The proposed TyI1a reaction intermediate (**20**), the degradation product (**19**), and the TyI1a reaction product (**7**) are shown.

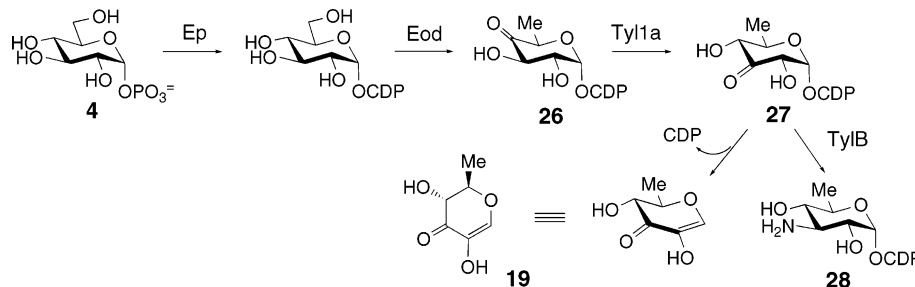
to *tylB* and exhibits a modest degree of sequence homology (34% identical and 52% similar) to a recently reported TDP-4-keto-6-deoxy-D-glucose-3,4-ketoisomerase (FdtA, catalyzing **6** → **18**; see the inset of Scheme 1) from the thermophilic bacillus species *Aneurinibacillus thermoaerophilus* (22). The FdtA enzyme is involved in S-layer polysaccharide biosynthesis and is the first hexose-3,4-ketoisomerase to be characterized biochemically. Subsequent heterologous expression of ORF *1a* (hereafter called *tyl1a*) together with *tylB*, *tylM1*, *tylM2*, and *tylM3* in the KdesI/VII *S. venezuelae* mutant resulted in the quantitative conversion of exogenously fed tylactone (**2**) to 5-O-mycaminosyltylactone (**10**, Scheme 2C). These findings identified TyI1a as the TDP-4-keto-6-deoxy-D-glucose-3,4-ketoisomerase in the mycaminoside pathway (Scheme 1) (8).

Herein, we report the overexpression, purification, and biochemical characterization of TyI1a. We showed via in

situ ¹H NMR spectroscopic analysis that TyI1a converts **6** to **7**, which can then be converted to **8** by incubation with the next enzyme in the mycaminoside pathway, TyIB. These results firmly establish TyI1a as the 3,4-ketoisomerase in the mycaminoside pathway. We also explored the substrate specificity of this enzyme and demonstrated that TyI1a processes the alternate substrate TDP-4-keto-2,6-dideoxy-D-glucose (**22**, Scheme 4) and can also act on CDP-4-keto-6-deoxy-D-glucose (**26**, Scheme 5), albeit at a much reduced rate. Additionally, we demonstrated that TyIB is able to convert the TyI1a products generated using **22** and **26** to TDP-3-amino-2,3,6-trideoxy-D-glucose (**25**, Scheme 4) and CDP-3-amino-3,6-dideoxy-D-glucose (**28**, Scheme 5), respectively. These findings have important implications for deoxysugar pathway engineering efforts and for the functional elucidation and characterization of other TyI1a and FdtA homologues.

Scheme 4: Enzymatic Synthesis of **22** Using **5**, RfbB, TylX3, and SpnN and Conversion of **22** to **25** Using Tyl1a and TylB^a

^a The Tyl1a reaction product (**23**) and the degradation product (**24**) are shown.

Scheme 5: Enzymatic Synthesis of **26** and Its Conversion to **28** by Tyl1a and TylB^a

^a The Tyl1a reaction product (**27**) and the degradation product (**19**) are shown.

EXPERIMENTAL PROCEDURES

Materials. The *tyl1a* and *tylB* genes were amplified from cosmid pSET552, generously provided by E. Seno of Eli Lilly Research Laboratories. *Escherichia coli* strain DH5 α and *Salmonella enterica* serovar Typhimurium LT2 (ATCC 15277) were purchased from Bethesda Research Laboratories (Gaithersburg, MD) and the American Type Culture Collection (Manassas, VA), respectively. Vector pET28b(+) and overexpression hosts *E. coli* BL21 and BL21(DE3) were purchased from Novagen (Madison, WI). Enzymes and molecular weight standards used for molecular cloning experiments were products of Invitrogen (Carlsbad, CA) or New England Biolabs (Ipswich, MA). Ni-NTA agarose and kits for DNA gel extraction and spin miniprep were obtained from Qiagen (Valencia, CA). *pfu* DNA polymerase was purchased from Stratagene (La Jolla, CA), and growth medium components were acquired from Becton Dickinson (Sparks, MD). Antibiotics and chemicals were products of Sigma-Aldrich Chemical Co. (St. Louis, MO) or Fisher Scientific (Pittsburgh, PA). Bio-gel P2 resin and all reagents for sodium dodecyl sulfate–polyacrylamide gel electrophoresis (SDS–PAGE) were purchased from Bio-Rad (Hercules, CA), with the exception of the prestained protein molecular weight marker, which was obtained from New England Biolabs. Amicon YM-10 filtration products were purchased from Millipore (Billerica, MA). Sephadex G-10 resin was acquired from Amersham (Piscataway, NJ). The CarboPac PA1 HPLC column was obtained from Dionex (Sunnyvale, CA), and Mono-Q H/R 16/10 and Superdex 200 HR 10/30 FPLC columns were obtained from Pharmacia (Uppsala, Sweden). Oligonucleotide primers for cloning of Tyl1a were prepared by Integrated DNA Technologies (Coralville, IA).

General. Protein concentrations were determined using the method of Bradford (23) using bovine serum albumin as the standard. The relative molecular mass and purity of enzyme samples were determined using SDS–PAGE as described

by Laemmli (24). The native molecular mass of Tyl1a was determined by the gel filtration method of Andrews (25). NMR spectra were acquired on either a Varian Unity 300 or 500 MHz spectrometer, and chemical shifts (δ in parts per million) are reported relative to that of dimethyl sulfoxide (DMSO, δ 2.54 for ¹H NMR). DNA sequencing was performed by the Core Facilities of the Institute of Cellular and Molecular Biology at the University of Texas. Mass spectra were obtained by the Mass Spectrometry Core Facility in the Department of Chemistry and Biochemistry at the University of Texas. The general methods and protocols for recombinant DNA manipulations followed those described by Sambrook et al. (26). Kinetic data were analyzed by nonlinear fit using Graft5 (Erithacus Software Ltd.).

Gene Amplification and Cloning of *tyl1a*. Two oligonucleotide primers complementary to the sequence at each end of *tyl1a* were prepared to amplify the *tyl1a* gene from the pSET552 cosmid. These two primers, Tylorfla-24/28-N-up (5'-GGAATTC**CA**TATGCGGCGAGCACTACGACGGAGGG-3') and Tylorfla-28-H-down (5'-GCG**CAAGCTT**CACGGGTGGCTCCTGCC-3'), were designed to amplify *tyl1a* with engineered 5' *Nde*I and 3' *Hind*III restriction sites (shown in bold) to be cloned into pET28b(+) and thereby encode expression of Tyl1a with an N-terminal His₆ tag. The PCR-amplified *tyl1a* gene was purified, digested with *Nde*I and *Hind*III restriction enzymes, and ligated into the *Nde*I–*Hind*III-digested vector, pET28b(+), to give recombinant plasmid *tyl1a*/pET28b(+). This plasmid was used to transform *E. coli* BL21 for protein overexpression.

Growth of *E. coli* BL21-*tyl1a*/pET28b(+) Cells. An overnight culture of *E. coli* BL21-*tyl1a*/pET28b(+) grown in Luria-Bertani (LB) medium containing 50 μ g/mL kanamycin at 37 °C was used (2 mL each) to inoculate 6 L (in 6 \times 1 L aliquots) of LB culture containing 35 μ g/mL kanamycin. These cultures were incubated at 37 °C until the

Cleavage of the N-His₆ Tag from Tyl1a by Thrombin. Tyl1a expressed from pET28b(+) contains a thrombin cleavage site between the His₆ tag and the first amino acid of Tyl1a. The Novagen thrombin cleavage capture kit containing biotinylated thrombin and straptavidin agarose for

Preparation of Enzymes Used To Synthesize TDP-4-Keto-6-deoxy-d-glucose (**6**). The TK, TMK, and NDK used in this synthesis were prepared as described by Takahashi et al. (9). Rabbit muscle pyruvate kinase was purchased from Sigma as a 400–800 units/mg ammonium sulfate precipitate. This ammonium sulfate precipitate was dissolved in water to a concentration of 2500 units/mL, dialyzed against 50 mM NaH₂PO₄ buffer and 300 mM NaCl (pH 8.0) to remove ammonium sulfate, and stored at –80 °C. RfbA was prepared as follows. The *rfbA* gene was amplified from *Sa. enterica* serovar Typhimurium LT2 genomic DNA using PCR. The start primer contained an engineered *Bam*HI restriction site (in *italics*), a ribosomal binding sequence (underlined), and an AT rich region upstream of the native start codon (shown in **bold**), with the sequence 5'-CGGGATCCGAAG-GAGATATATAATGAAAACGCGTAAGGC-3'. The halt primer contained an engineered *Pst*I restriction site (in *italics*) and a C-terminal His₅ tag (underlined) immediately downstream of the stop codon (in **bold**), with the sequence 5'-CTTGCAATGCCTGCAGTTAATGATGATGATGATGTAAACCTTTCACCATC-3'. The PCR-amplified gene was purified, digested with *Bam*HI and *Pst*I, and ligated into *Bam*HI–*Pst*I-digested pUC18. The resulting construct was used to transform *E. coli* BL21(DE3). Overexpression was achieved by growing the transformed host in LB medium in the presence of 100 µg/mL ampicillin at 37 °C overnight. Protein was purified from the harvested cells by Ni-NTA affinity chromatography in a manner identical to that used for purification of Ty11a. RfbB used in the synthesis of **6** was prepared in the following manner. The *rfbB* gene was amplified from *Sa. enterica* serovar Typhimurium LT2 genomic DNA by PCR. The start primer contained an engineered *Eco*RI restriction site (in *italics*), a ribosomal binding sequence (underlined), and an AT rich region upstream of the native start codon (shown in **bold**), with the sequence 5'-GGAATTCTGAAGGAGATATATAATGGT-GAAGATACTTATTACTGG-3'. The halt primer contained an engineered *Bam*HI restriction site (in *italics*) and a His₅

tag sequence (underlined) immediately downstream of the stop codon (in bold), with the sequence 5'-CGGGATCCT-TAATGATGATGATGATGCTGGCGTCCTTCATAGTTC-3'. The PCR-amplified gene was purified, digested with *EcoRI* and *BamHI*, and ligated into *EcoRI*-*BamHI*-digested pUC18. The resulting construct was used to transform *E. coli* BL21(DE3). Overexpression was achieved by growth of the transformed host in LB medium supplemented with 100 μ g/mL ampicillin at 37 °C overnight. Protein was purified from the harvested cells by Ni-NTA affinity chromatography in a manner identical to that used for the purification of Tyl1a.

Enzymatic Synthesis of TDP-4-Keto-6-deoxy-D-glucose (6). The large-scale enzymatic preparation of Tyl1a substrate was initiated by coupling thymidine with glucose 1-phosphate (4) to make TDP-D-glucose (5), which was then converted to TDP-4-keto-6-deoxy-D-glucose (6). Preparation of TDP-D-glucose from thymidine and glucose 1-phosphate (4) was conducted in a two-stage, "one-pot" reaction (9). In the first stage, a mixture containing 76.2 mM phosphoenolpyruvate (PEP), 24 mM thymidine, 1.6 mM ATP, 27 mM MgCl₂, 25 μ M thymidine kinase (TK), 25 μ M thymidylate kinase (TMK), 25 μ M nucleoside diphosphate kinase (NDK), and 1000 units of rabbit muscle pyruvate kinase (PK) in 17 mL of 45 mM Tris-HCl buffer (pH 7.5) was incubated at 37 °C for 4 h, generating thymidine triphosphate (TTP). The enzymes were removed by filtration through an Amicon YM-10 membrane, and glucose 1-phosphate (4), MgCl₂, and α -D-glucose-1-phosphate thymidyltransferase (RfbA) from *Sa. enterica* LT2 were added to the filtrate to give final concentrations of 28 mM, 50 mM, and 36 μ M, respectively. The mixture was incubated for 16 h at 37 °C, centrifuged at 5000g for 10 min to remove the precipitate, and filtered through an Amicon YM-10 membrane to remove enzymes. The crude product (5), with a theoretical yield of 228 mg, was stored at 4 °C.

The enzyme-free filtrate from the previous step was loaded onto a Bio-gel P2 column (25 mm \times 100 cm) prewashed with water and run at a flow rate of 12 mL/h with water as the eluant, with 8 mL fractions collected. Fractions exhibiting UV absorption at 267 nm were lyophilized, and the identity and purity of the compounds in each fraction were assessed by ¹H and ³¹P NMR spectroscopy. TDP-D-glucose (5)-containing fractions (total weight of 170 mg), which varied in purity from 25 to 70%, were pooled according to their purities. Further purification of TDP-D-glucose was performed with a FPLC system equipped with a Mono Q 16/10 column. A linear gradient of 0 to 40% of a solution of 400 mM NH₄HCO₃ in water was used as the eluant. The detector was set at 280 nm, and the flow rate was 5 mL/min. Fractions containing the major peak were lyophilized individually, redissolved in water, and lyophilized again to remove NH₄HCO₃. The purities of these fractions (total weight of 123 mg), which ranged from 50 to 90%, were assessed by ¹H and ³¹P NMR spectroscopy. From these fractions, 23 mg of 90% pure TDP-D-glucose (5) was obtained. ¹H NMR (300 MHz, D₂O): δ 1.78 (3H, s, 5''-Me), 2.22 (2H, m, 2'-H), 3.28–3.40 (2H, m, 2-H, 3-H), 3.59–3.78 (2H, m, 4-H, 5-H), 3.95–4.06 (3H, m, 4'-H, 5'-H), 4.45 (1H, m, 3'-H), 5.44 (1H, dd, J = 6.9, 3.3 Hz, 1-H), 6.20 (1H, t, J = 6.9 Hz, 1'-H), 7.59 (1H, s, 6''-H).

TDP-D-glucose (5, 23 mg) obtained from the previous step was dissolved in 47 mM KH₂PO₄ buffer (pH 7.5) to give a final concentration of 29 μ M. This solution was incubated with TDP-D-glucose 4,6-dehydratase (RfbB) from *Sa. enterica* LT2 (18 μ M) at 37 °C for 2 h, after which RfbB was removed by filtration through an Amicon YM-10 membrane. The filtrate was loaded onto a Sephadex G-10 column prewashed with water and run at a flow rate of 1 mL/min using water as the eluant, with 10 mL fractions collected. Those fractions exhibiting absorption at 267 nm were lyophilized and their purities assessed by ¹H and ³¹P NMR spectroscopy. Those fractions containing pure TDP-4-keto-6-deoxy-D-glucose (6, 12.3 mg, >90% pure) were combined, and the concentration of 6 in the solution was determined spectrophotometrically at 267 nm (ϵ = 9600 M⁻¹ cm⁻¹). ¹H NMR (300 MHz D₂O) of 6 (a mixture of hydrate and keto forms): δ 1.08 (3H, d, J = 6.5 Hz, 5-Me of the hydrate form), 1.12 (3H, d, J = 6.5 Hz, 5-Me of the keto form), 1.79 (3H, s, 5''-Me), 2.09–2.26 (2H, m, 2'-H), 3.48 (1H, m, 2-H of the hydrate form), 3.64 (1H, d, J = 10.0 Hz, 3-H of the hydrate form), 3.68 (1H, m, 2-H of the keto form), 3.96 (1H, q, J = 6.5 Hz, 5-H of the hydrate form), 4.01–4.07 (3H, m, 4'-H, 5'-H), 4.48 (1H, m, 3'-H), 5.41 (1H, dd, J = 7.3, 3.8 Hz, 1-H of the hydrate form), 5.59 (1H, dd, J = 7.0, 3.0 Hz, 1-H of the keto form), 6.20 (1H, t, J = 6.9 Hz, 1'-H), 7.60 (1H, s, 6''-H).

Enzymatic Preparation of TDP-4-Keto-2,6-dideoxy-D-glucose (22). This compound was prepared enzymatically from TDP-D-glucose (5) using purified enzymes RfbB from *Sa. enterica* LT2, TylX3 from *S. fradiae* (27), and SpnN, the TDP-3,4-diketo-2,6-dideoxy-D-glucose-3-ketoreductase from the spinosyn biosynthetic pathway of *Saccharopolyspora spinosa* (28) (Scheme 4). A typical reaction mixture containing 28 mM TDP-D-glucose (5), 34 μ M RfbB, 17 mM NADPH, 10 μ M TylX3, 17 μ M SpnN, in 50 mM Tris-HCl buffer (pH 7.5), and 10% glycerol was incubated at 25 °C for 4 h. Enzymes were removed using a Centricon YM-10 microconcentrator, and the filtrate was separated on a Bio-gel P2 gel filtration column (25 mm \times 100 cm) prewashed with 25 mM NH₄HCO₃ and run at a flow rate of 12 mL/h with 25 mM NH₄HCO₃ as the eluant. Fractions (8 mL each) exhibiting UV absorbance at 267 nm were lyophilized, and the identity and purity of the compounds in each fraction were assessed by ¹H and ³¹P NMR spectroscopy. The ¹H NMR spectrum of the purified TDP-4-keto-2,6-dideoxy-D-glucose (22) was identical to that previously reported (29).

HPLC Activity Assay for Tyl1a. A reaction mixture (35 μ L) containing 2.85 μ M Tyl1a (with or without the N-His₆ tag) and 1 mM TDP-4-keto-6-deoxy-D-glucose (6) in 50 mM KH₂PO₄ buffer (pH 7.5) was incubated at 25 °C. Aliquots (5 μ L) were removed at various time points, quenched by being flash-frozen in liquid nitrogen, thawed at 4 °C, diluted by addition of 20 μ L of 50 mM KH₂PO₄ buffer (pH 7.5), and filtered through a Microcon YM-10 membrane to remove enzyme, and the filtrate was flash-frozen until HPLC analysis. HPLC analysis was performed using a Dionex CarboPac PA1 column with 9.5 μ L of sample for each injection. The sample was eluted with a gradient of water as solvent A and 500 mM NH₄OCOCH₃ (adjusted to pH 7.0 with aqueous NH₃) as solvent B where the gradient ran from 5 to 20% B over 15 min, from 20 to 60% B over 20 min, from 60 to 100% B over 2 min, with a 3 min wash at

100% B, and from 100 to 5% B over 5 min, followed by re-equilibration at 5% B for 15 min. The flow rate was 1 mL/min, and the detector was set at 267 nm. The retention times were 35.3 min for TDP-4-keto-6-deoxy-D-glucose (**6**), 39.0 min for TDP-3-keto-6-deoxy-D-glucose (**7**), 41.9 min for TDP, and 1.8 min for the degradation product, (2*R*,3*R*)-2-methyl-3,5-dihydroxy-4-keto-2,3-dihydropyran (**19**). The substrate and product ratios were calculated from the integration of the corresponding peaks on the HPLC chromatogram.

In Situ ¹H NMR Assay for Tyl1a and Characterization of Products. A reaction mixture (600 μ L) containing 10 mM TDP-4-keto-6-deoxy-D-glucose (**6**), 50 mM KH₂PO₄ buffer (pH 7.5), and 5% (v/v) DMSO-*d*₆ (as a reference) was prepared in a NMR tube. After shimming and initial peak integration in a 500 MHz NMR spectrometer, the sample was removed from the tube, mixed thoroughly with glycerol-free His₆-tagged Tyl1a (final concentration of 6 or 10 μ M), and returned to the NMR tube. Data were acquired at 5 min intervals for 150 min. Spectral data for TDP-3-keto-6-deoxy-D-glucose (**7**) and the degradation product (2*R*,3*R*)-2-methyl-3,5-dihydroxy-4-keto-2,3-dihydropyran (**19**) were assigned from the spectra generated during the *in situ* assay. ¹H NMR (DMSO-*d*₆) of **7**: δ 1.23 (3H, d, *J* = 5.5 Hz, 5-Me), 1.73 (3-H, s, 5'-Me), 2.15–2.20 (2H, m, 2'-H), 3.92–4.01 (5H, m, 4-H, 5-H, 4'-H, 5'-H), 4.00–4.05 (1H, m, 2-H), 4.45–4.50 (1H, m, 3'-H), 5.68 (1H, dd, *J* = 7.0, 4.5 Hz, 1-H), 6.15 (1H, t, *J* = 7.0 Hz, 1'-H), 7.55 (1H, s, 6''-H). ¹H NMR (DMSO-*d*₆) of **19**: δ 1.28 (3H, d, *J* = 6.0 Hz, 5-Me), 4.03 (1H, d, *J* = 12.3 Hz, 4-H), 4.10 (1H, dq, *J* = 12.3, 6.0 Hz, 5-H), 7.32 (1H, s, 1-H).

Determination of Kinetic Parameters for Tyl1a. The steady state kinetic parameters of the Tyl1a-catalyzed reaction were determined by the HPLC activity assay as described above. Reaction mixtures containing 100 nM N-His₆-tagged Tyl1a and varied amounts of TDP-4-keto-6-deoxy-D-glucose (**6**) (3 μ M to 1 mM) in 50 mM KH₂PO₄ buffer (pH 7.5) were incubated at 25 °C. Larger reaction volumes were used for the lower substrate concentrations to facilitate HPLC analysis. Aliquots were taken at four different time points for each of 16 substrate concentrations. Incubation mixtures with lower substrate concentrations were monitored for shorter periods of time (2–3 min), and those with higher substrate concentrations were monitored for periods as long as 7 min. Since the concentration of substrate in each sample was known, the percent conversion determined by HPLC could be used to calculate the micromoles of product formed for each time point. The amounts of product formed at the four time points for a given substrate concentration were plotted against time, and the slope of each line was plotted versus substrate concentration. The resulting data were fit to the Michaelis–Menten equation by nonlinear regression using Grafit 5 to determine the *k*_{cat} and *K*_m values.

As a comparison, data obtained from the HPLC time course study and those obtained from the *in situ* NMR assay by following changes in integration of individual proton signals over time (for example, the 5-methyl signal of **6** and **7** and the 2-methyl signal of **19**) were also used to calculate the apparent *k*_{cat}. In each case, peak integrations were normalized to initial substrate concentration, and data sets were individually fit to either single- or double-exponential equations by nonlinear regression analysis using Grafit 5.

The rate constant for the disappearance of substrate from these data was used to calculate the apparent *k*_{cat} in each experiment.

HPLC Assay of the Coupled Tyl1a–TylB Reaction. The C-3 aminotransferase TylB (**18**) used in this coupled assay and the TylB product standard, TDP-3-amino-3,6-dideoxy-D-glucose (**8**) (**16**), were prepared according to published procedures. The reaction mixture (100 μ L) contained 28.5 μ M Tyl1a, 10 μ M TylB, 1 mM TDP-4-keto-6-deoxy-D-glucose (**6**), 10 mM L-glutamate, and 50 μ M pyridoxal 5'-phosphate (PLP), in 50 mM KH₂PO₄ buffer (pH 7.5). Aliquots were removed at various time points and analyzed by HPLC in the same manner that was used for Tyl1a activity assays. The HPLC retention time for TDP-3-amino-3,6-dideoxy-D-glucose (**8**) was 13.7 min. For isolation and MS characterization of the TylB product (**8**) and Tyl1a degradation product (**19**), 300 μ g of TDP-4-keto-6-deoxy-D-glucose (**6**) at a concentration of 1 mM was incubated with 3 μ M Tyl1a, 10 μ M TylB, 50 μ M PLP, and 10 mM L-glutamate in 50 mM KH₂PO₄ buffer (pH 7.5). The total reaction volume was 550 μ L. The reaction mixture was incubated at 25 °C for 70 min, the reaction quenched by flash-freezing in liquid nitrogen, and the mixture thawed on ice, and enzymes were removed by filtration through Microcon YM-10 at 4 °C. The sample was then separated using a semipreparative Dionex CarboPac PA-1 column and a gradient elution program identical to that used for the analytical Dionex CarboPac PA-1 column, with a flow rate of 5 mL/min. Compounds **8** and **19**, which eluted at 12.5 and 1.8 min, respectively, were collected manually and lyophilized to dryness. HPLC analysis showed 35% conversion of **6** to **8** and 65% conversion of **6** to **19** (the degradation product) and TDP. Compound **8** was resuspended in water to a concentration of 0.1 mg/mL, and **19** was resuspended in methanol to a concentration of 1 mg/mL. High-resolution ESI-MS of **8**: calcd for C₁₆H₂₇N₃O₁₄P₂ (*M* – H) 546.0883, found 546.0885. High-resolution ESI-MS of **19**: calcd for C₆H₄O₄ (*M* + H) 145.0501, found 145.0500.

*HPLC Analysis of the Incubation Mixture Containing Tyl1a with TDP-4-Keto-2,6-dideoxy-D-glucose (**22**).* The reaction mixture (70 μ L) contained 2.85 μ M Tyl1a and 1 mM **22** in 50 mM KH₂PO₄ buffer (pH 7.5) and was incubated at 25 °C. Aliquots were removed at various time points and analyzed by HPLC in the same manner that was used for other Tyl1a activity assays. The retention time of substrate **22** was 33.4 min; that of the product, TDP-3-keto-2,6-dideoxy-D-glucose (**23**), was 37.0 min, and that of the degradation product, (2*R*,3*R*)-2-methyl-3-hydroxy-4-keto-2,3-dihydropyran (**24**), was 1.7 min. Peak integrations were normalized to initial substrate concentration, and data sets were individually fit to either single- or double-exponential equations by nonlinear regression analysis using Grafit 5. The rate constant for the disappearance of substrate obtained from these data was used to calculate the apparent *k*_{cat} in each experiment.

*Coupled Assay of Tyl1a–TylB with TDP-4-Keto-2,6-dideoxy-D-glucose (**22**).* The reaction mixture (50 μ L), which was incubated at 25 °C, contained 2.85 μ M Tyl1a, 28.5 μ M TylB, 1 mM **22**, 28.5 mM L-glutamate, and 142.5 μ M PLP in 50 mM KH₂PO₄ buffer (pH 7.5). Aliquots were removed at various time points and subjected to HPLC analysis as described for the Tyl1a activity assays. The retention time

of the product, TDP-3-amino-2,3,6-trideoxy-D-glucose (**25**), was 9.5 min. For isolation and MS characterization of the Ty1B product (**25**) and Ty1a degradation product (**24**), 1.0 mg of the SpnN product TDP-4-keto-2,6-dideoxy-D-glucose (**22**) at a concentration of 2 mM was incubated with 1 μ M Ty1a, 30 μ M Ty1B, 250 μ M PLP, and 50 mM L-glutamate in 50 mM KH_2PO_4 buffer (pH 7.5). The total reaction volume was 940 μ L. The reaction mixture was incubated at 25 °C for 12 h, and enzymes were removed by filtration through Microcon YM-10 at 4 °C. The sample was then separated using a semipreparative Dionex CarboPac PA-1 column and a gradient elution program identical to that used for the analytical Dionex CarboPac PA-1 column, with a flow rate of 5 mL/min. Compounds **25** and **24**, which eluted at 8.9 and 1.8 min, respectively, were collected. HPLC analysis showed 15% conversion of **22** to **25** and 85% conversion of **22** to **24** (the degradation product) and TDP. Compound **24** was lyophilized to dryness and resuspended in methanol to a concentration of 1 mg/mL. Compound **25**, which is unstable when lyophilized to dryness or when stored at 25 °C, was lyophilized to reduce its volume 10-fold and stored at -80 °C. High-resolution EI-MS of **24**: calcd for $\text{C}_6\text{H}_4\text{O}_3$ (M^+) 128.0473, found 128.0486. High-resolution ESI-MS of **25**: calcd for $\text{C}_{16}\text{H}_{27}\text{N}_3\text{O}_{13}\text{P}_2$ ($\text{M} - \text{H}$) 530.0941, found 530.0941.

HPLC Analysis of the Incubation Mixture Containing Ty1a and CDP-4-Keto-6-deoxy-d-glucose (26). Preparation and quantitation of CDP-4-keto-6-deoxy-D-glucose (**26**) was conducted as described by Chen et al. (30). Preparation of enzymes used to make **26** was performed as described by Thorson et al. (31, 32). The reaction mixture (100 μ L) contained 100 μ M Ty1a and 1 mM **26** in 50 mM KH_2PO_4 buffer (pH 7.5), and the incubation was carried out at 25 °C. Aliquots were removed at various time points and analyzed by HPLC in the same manner that was used for other Ty1a activity assays. The retention times of **26**, the product CDP-3-keto-6-deoxy-D-glucose (**27**), and CDP were 33.1, 36.6, and 42.3 min, respectively. Peak integrations were normalized to initial substrate concentration, and data sets were individually fit to either single- or double-exponential equations by nonlinear regression analysis using Grafit 5. The rate constant for the disappearance of substrate obtained from these data was used to calculate the apparent k_{cat} in each experiment.

Coupled Assay of Ty1a and Ty1B with CDP-4-Keto-6-deoxy-d-glucose (26). The reaction mixture (100 μ L), which was incubated at 25 °C, contained 35 μ M Ty1a, 35 μ M Ty1B, 1 mM **26**, 35 mM L-glutamate, and 175 μ M PLP in 50 mM KH_2PO_4 buffer (pH 7.5). Aliquots were removed at various time points and subjected to HPLC analysis as described for the Ty1a activity assays. The retention time of the product, CDP-3-amino-3,6-dideoxy-D-glucose (**28**), was 11.4 min. For isolation and MS characterization of the Ty1B product (**28**), 1.8 mM CDP-4-keto-6-deoxy-D-glucose (**26**) was incubated with 35 μ M Ty1a, 35 μ M Ty1B, 175 μ M PLP, and 35 mM L-glutamate in 100 μ L of 50 mM KH_2PO_4 buffer (pH 7.5). The reaction mixture was incubated at 25 °C for 48 h, and enzymes were removed by filtration using a Microcon YM-10 at 4 °C. The sample was then further purified using a semipreparative Dionex CarboPac PA-1 column and a gradient elution program identical to that used for the analytical Dionex CarboPac PA-1 column, with a flow rate of 5 mL/min. Compound **28**, which was eluted

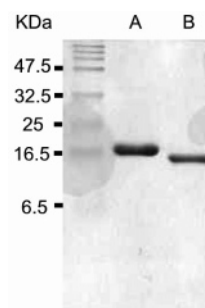


FIGURE 1: SDS-PAGE gel (18%) of (A) purified N-His₆-tagged Ty1a and (B) purified Ty1a with the His₆ tag removed by thrombin cleavage.

at 11.1 min, was collected manually, lyophilized to dryness, and resuspended in water to a concentration of 0.1 mg/mL. High-resolution ESI-MS of **28**: calcd for $\text{C}_{15}\text{H}_{25}\text{N}_4\text{O}_{14}\text{P}_2$ ($\text{M} - \text{H}$) 547.0843, found 547.0841. HPLC analysis showed 46% conversion of **26** to **28**, with the remaining 54% consisting of **26** and **27**.

RESULTS

Purification and Characterization of Ty1a. The *tyl1a* gene (33) was amplified, cloned, and overexpressed to give N-terminally His₆-tagged Ty1a. Production of soluble protein was quite efficient, with 275 mg of Ty1a obtained from a 6 L culture after the Ni-NTA chromatographic step. Further purification by FPLC using a Mono Q column improved the purity to >95% as assessed by SDS-PAGE. The subunit molecular mass was estimated to be 19 kDa on the basis of SDS-PAGE analysis (Figure 1), which agrees well with the calculated mass of 18 806 Da for the N-terminal methionine-cleaved His₆-tagged Ty1a. Thrombin cleavage was also carried out to generate Ty1a without the N-terminal His₆ tag for comparative kinetic studies. Gel filtration analysis revealed a native molecular mass of 31.0 kDa for Ty1a, suggesting a homodimeric structure in solution.

Catalytic Properties of Ty1a. Because Ty1a exhibits a modest degree of sequence identity (34% identical and 52% similar) with FdtA, which catalyzes the conversion of TDP-4-keto-6-deoxy-D-glucose (**6**) to TDP-3-keto-6-deoxy-D-galactose (**18**) (22), we hypothesized that Ty1a might also be a hexose 3,4-ketoisomerase catalyzing a similar reaction in the mycaminose pathway. The predicted substrate of Ty1a, TDP-4-keto-6-deoxy-D-glucose (**6**), was therefore prepared enzymatically from thymidine and glucose 1-phosphate (**4**) using six enzymes in a two-stage, one-pot reaction (9). Subsequent HPLC analysis of an incubation mixture containing **6** and N-His₆-tagged Ty1a showed time-dependent depletion of substrate and the appearance of three new products (Figure 2A, traces a and b). Identical results were also observed using thrombin-cleaved Ty1a under the same reaction conditions, indicating that the N-terminal His₆ tag has no effect on Ty1a activity. Thus, the N-His₆-tagged Ty1a was used for all subsequent work. Analysis of the full reaction time course revealed that **6** (retention time of 35.3 min) was first converted to an intermediate (retention time of 39.0 min), which was swiftly depleted with concomitant formation of TDP (retention time of 41.9 min) and a new product (retention time of 1.8 min) (Figure 2B). Integration of the peak corresponding to the substrate and each of the three new peaks over time gave the traces shown in Figure

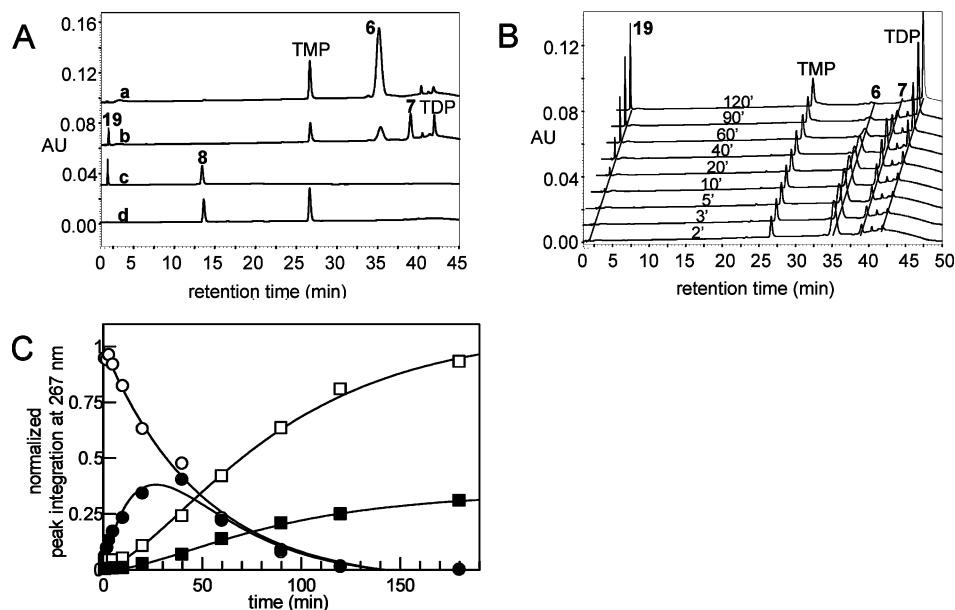


FIGURE 2: (A) HPLC traces showing product formation in the TyIIa and TyIIb reactions: (a) incubation mixture containing TDP-4-keto-6-deoxy-D-glucose (**6**, 1 mM) in 50 mM KH₂PO₄ buffer (pH 7.5) without TyIIa, (b) incubation mixture containing **6** (1 mM) and TyIIa (2.85 μM) in the same phosphate buffer described for trace a, (c) incubation mixture containing **6** (1 mM) and TyIIa (28.5 μM) in the presence of TyIIb (10 μM), PLP (50 μM), and L-glutamate (10 mM), in the same phosphate buffer described for trace a (note that TMP and TDP peaks are not visible due to the adjustment of the scaling to keep the strong peaks of **8** and **19** in scale), and (d) chemically synthesized TDP-3-amino-3,6-dideoxy-D-glucose (**8**). (B) HPLC traces of the TyIIa reaction time course study (2–120 min) using 1 mM **6** and 2.85 μM TyIIa in 50 mM KH₂PO₄ buffer (pH 7.5). (C) Time course of the TyIIa (2.85 μM)-catalyzed reaction using **6** (1 mM) as the substrate. Integrations of the HPLC peaks of substrate, product, and degradation products are plotted vs time: (○) **6**, (●) **7**, (■) **19**, and (□) TDP (see Experimental Procedures for details).

2C. Evidently, the immediate product having a retention time of 39.0 min is unstable, degrading to TDP and a new species with a retention time of 1.8 min. In an attempt to divert the transient intermediate to a more stable product, TyIIb, which catalyzes the subsequent step in the mycaminose pathway, was added to the incubation mixture. As expected, the addition of TyIIb along with PLP and L-glutamate to the reaction mixture led to a new product (retention time of 13.7 min), which coeluted with the chemically synthesized TDP-3-amino-3,6-dideoxy-D-glucose (**8**) (Figure 2A, traces c and d). The identity of this new product was further confirmed to be **8** by high-resolution ESI mass spectrometry. Clearly, the unstable intermediate generated in the TyIIa reaction is TDP-3-keto-6-deoxy-D-glucose (**7**), which is converted to **8** in the presence of TyIIb.

In Situ ¹H NMR Analysis of TyIIa Reaction and Identification of Reaction Products. To directly characterize the unstable TyIIa reaction product, *in situ* ¹H NMR analysis was performed. In this experiment, TDP-4-keto-6-deoxy-D-glucose (**6**) was incubated with glycerol-free TyIIa in a NMR tube, and the reaction was monitored at 5 min intervals for 150 min. A stack plot of the resulting spectra in which 6 μM TyIIa was used is shown in Figure 3. Disappearance of the proton signals for **6** is seen along with the appearance of a new set of signals for the TyIIa product. These signals reached a maximum intensity at ~50 min and then diminished. A third set of signals corresponding to the degradation product also appeared after a short lag. Comparison of these spectra to those of **6** and the chemoenzymatically synthesized **7** (**18**) enabled assignment of the ¹H NMR signals for **7**. Thus, the TyIIa product is indeed TDP-3-keto-6-deoxy-D-glucose (**7**) which confirms that TyIIa is a TDP-4-keto-6-deoxy-D-glucose-3,4-ketoisomerase. Signals corresponding to the degradation product were also identified. The chemical

shifts and coupling constants of these signals are consistent with the structure of (2*R*,3*R*)-2-methyl-3,5-dihydroxy-4-keto-2,3-dihydropyran (**19**), which is likely formed by C-2 deprotonation of **7** followed by elimination of TDP to give the 1,2-unsaturated ketone (Scheme 3). High-resolution CI-MS analysis of the 1.8 min peak collected from the HPLC assay confirms the assigned structure.

Determination of Kinetic Parameters for TyIIa-Catalyzed Reaction. To determine the steady state kinetic parameters for the TyIIa-catalyzed conversion of **6** to **7**, a discontinuous HPLC assay was developed and performed. The plot of v_0 (initial velocity) versus [S] (3 μM to 1 mM) (Figure 4A) was fitted to the Michaelis–Menten equation by nonlinear regression to yield a k_{cat} of 6.1 min⁻¹ and a K_m of 27 μM for **6**. Data obtained by fitting the experimental data from the HPLC time course study (Figure 2C) and those obtained from the *in situ* NMR assay (Figure 4B) by nonlinear regression using single- or double-exponential equations were also used to calculate apparent k_{cat} values. A k_{cat} of ~7.0 min⁻¹ was obtained from the HPLC data, and an apparent k_{cat} of 2.4 ± 0.6 min⁻¹ was obtained from the *in situ* ¹H NMR assays. These values are in good agreement with the k_{cat} value determined by the HPLC initial velocity assays.

TyIIa Substrate Specificity. To determine the substrate specificity of TyIIa, the 2-deoxy analogue of **6**, TDP-4-keto-2,6-dideoxy-D-glucose (**22**), and the CDP version of **6**, CDP-4-keto-6-deoxy-D-glucose (**26**), were tested as possible substrates. Compound **22** was prepared enzymatically from TDP-4-keto-6-deoxy-D-glucose (**6**) using TyIX3 (**27**) from the mycarose biosynthetic pathway of *S. fradiae* and SpnN (**28**) from the forosamine biosynthetic pathway of *S. spinosa* as the catalysts (Scheme 4). HPLC analysis of an incubation mixture containing **22** (1 mM) and TyIIa (2.85 μM) showed time-dependent disappearance of the substrate peak at 33.4

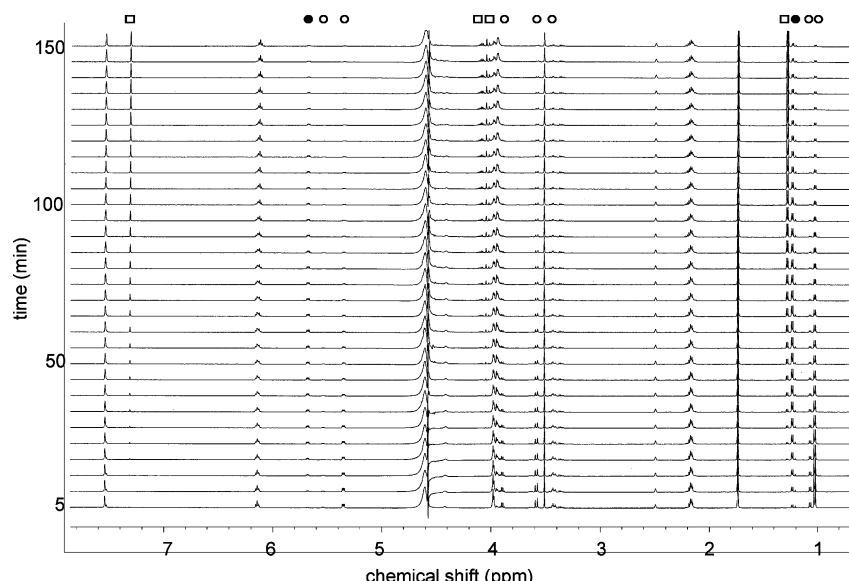


FIGURE 3: ^1H NMR stack plot of the Tyl1a reaction [10 mM **6** and 6 μM Tyl1a in 50 mM KH_2PO_4 buffer (pH 7.5)] monitored over 150 min. The signals corresponding to each compound are labeled: (○) from **6**, (●) from **7**, and (□) from **19** (see Experimental Procedures for details).

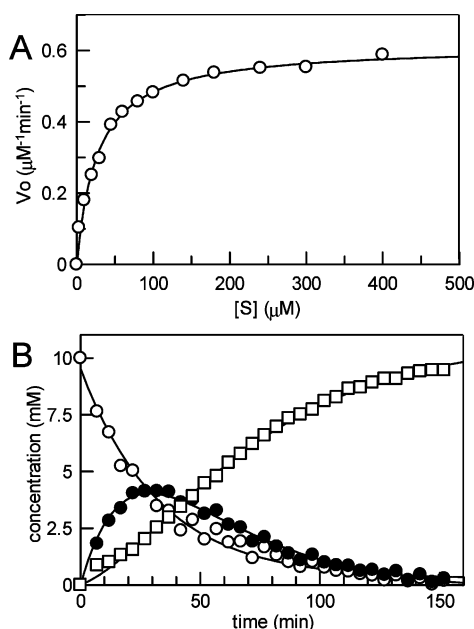


FIGURE 4: (A) Plot of v_0 vs $[S]$ determined via a HPLC assay from which the steady state kinetic constants for the Tyl1a reaction were determined. (B) Plot of the integration of the ^1H NMR signals (see Figure 3) of the 5-methyl group of **6** (○) and **7** (●) and that of the 2-methyl group of **19** (□) during the in situ ^1H NMR assay [10 mM **6** and 10 μM Tyl1a in 50 mM KH_2PO_4 buffer (pH 7.5)] (see Experimental Procedures for details).

min, accumulation of a small amount of a new peak at 37.0 min, and the tandem formation of TDP and another new peak at 1.7 min (Figure 5, traces a and b). On the basis of the retention times and confirmed identities of products from the assay of Tyl1a with **6**, the peaks at 37.0 and 1.7 min likely correspond to TDP-3-keto-2,6-dideoxy-D-glucose (**23**) and its degradation product (2*R*,3*R*)-2-methyl-3-hydroxy-4-keto-2,3-dihydropyran (**24**), respectively (Scheme 4). While no spectral data were collected for **23** due to its low yield and instability, high-resolution CI-MS data of the 1.7 min peak are consistent with the assigned structure of **24**. By plotting the peak integration of substrate, product, and

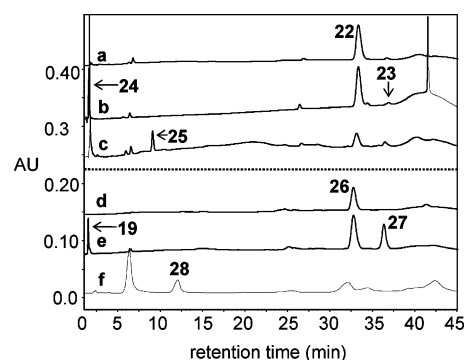


FIGURE 5: HPLC traces showing conversion of alternate substrates **22** and **26** by Tyl1a and TylB: (a) 1 mM **22** without Tyl1a, (b) 1 mM **22** with 2.85 μM Tyl1a, (c) 1 mM **22** with 2.85 μM Tyl1a, 28.5 μM TylB, 142.5 μM PLP, and 28.5 mM L-glutamate, (d) 1 mM **26** without Tyl1a, (e) 1 mM **26** with 100 μM Tyl1a, and (f) 1 mM **26** with 35 μM Tyl1a, 35 μM TylB, 175 μM PLP, and 35 mM L-glutamate.

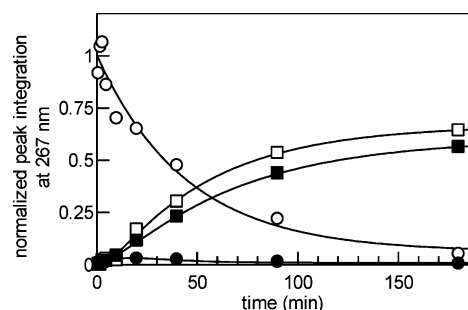


FIGURE 6: Time course of the Tyl1a (2.85 μM)-catalyzed reaction using **22** (1 mM) as a substrate. Integrations of the HPLC peaks of the substrate, product, and degradation products are plotted vs time: (○) **22**, (●) **23**, (■) **24**, and (□) TDP.

degradation products of this reaction versus time (Figure 6), we found that **23** is more prone to degradation than **7**, as less of it accumulates during the course of the reaction, and TDP and **24** are formed significantly more rapidly. By fitting the substrate depletion data from this time course to a single-

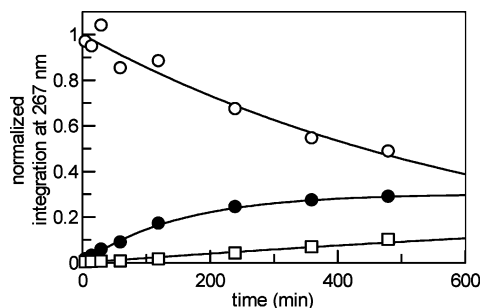


FIGURE 7: Time course of the TyllA (100 μ M)-catalyzed reaction using **26** (1 mM) as a substrate. Integrations of the HPLC peaks of the substrate, product, and degradation products are plotted vs time: (○) **26**, (●) **27**, and (□) **19**.

exponential equation, we estimated the apparent k_{cat} for the conversion of **22** to **23** by TyllA to be 7.9 min^{-1} (Figure 6). These analyses indicate that **22** and **6** are comparable substrates for TyllA.

We next examined whether TyllA can accept CDP-4-keto-6-deoxy-D-glucose (**26**) as a substrate. This compound was generated enzymatically from CTP and glucose 1-phosphate (**4**) by the action of α -D-glucose cytidyltransferase (E_p) and CDP-D-glucose 4,6-dehydratase (E_{od}) from *Yersinia pseudotuberculosis* as described previously (Scheme 5) (30). The assay was initially performed using 1 mM **26** and 1 μ M TyllA and monitored by HPLC. Although formation of a new peak at 36.6 min was discernible, its formation was very slow, with only 2% conversion observed after a 24 h incubation. The assay was repeated with an increased amount of TyllA (100 μ M), and the time-dependent disappearance of substrate at 33.1 min, the formation of product at 36.6 min, and the degradation of the product to TDP and a new product at 1.8 min were clearly noted, with product levels reaching a maximum of 30% conversion after 8 h (Figure 5, traces d and e). The pattern of product formation and degradation is similar to that observed for the TyllA reaction with its natural substrate, suggesting that the product in this case is likely CDP-3-keto-6-deoxy-D-glucose (**27**), and the degradation product seen at 1.8 min is the same pyran (**19**) formed in the reaction of TyllA with **6**. By fitting the substrate depletion data from this time course to a single exponential, we calculated the apparent k_{obs} value for the conversion of **26** to **27** by TyllA under these conditions to be 0.015 min^{-1} (Figure 7). Thus, TyllA appears to also be able to catalyze a 3,4-ketoisomerization of **26**, although the efficiency of conversion is low, requiring a high concentration of enzyme and a long incubation time to achieve significant turnover.

TyLB Substrate Specificity. Incubation of **22** with TyllA (2.85 μ M) and TyLB (28.5 μ M) was also carried out to test whether TyLB could accept **23** as a substrate. As expected, HPLC analysis of the incubation mixture showed substrate depletion as well as formation of the degradation products, TDP and **24**. Interestingly, the time-dependent formation of a new peak at 9.5 min was also observed. The level of conversion of **22** to this new species was less than 2% as estimated from peak integration. Inclusion of less TyllA (1 μ M) and more TyLB (50 μ M) along with a longer incubation time (12 h) resulted in a 15% overall conversion (Figure 5, trace c). In view of the effect of the increased TyLB concentration, this new product is likely TDP-3-amino-2,3,6-

trideoxy-D-glucose (**25**). High-resolution ESI-MS data of this product purified by HPLC are consistent with the assigned structure (**25**). These results strongly suggest that TyLB is capable of converting **23** to **25** in spite of the inherent instability of **23**.

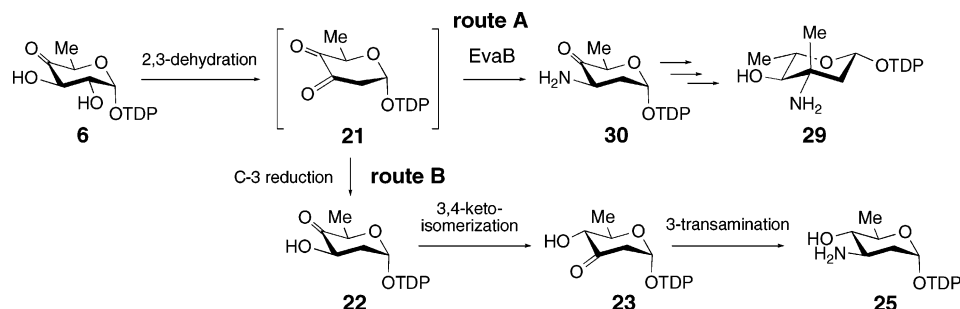
Encouraged by the observation that TyllA was able to convert **23** to **25**, we subsequently incubated CDP-4-keto-6-deoxy-D-glucose (**26**) (1 mM) with TyllA (35 μ M) and TyLB (35 μ M) to test the ability of TyLB to accept **27** as a substrate. As expected, we observed slow substrate depletion and concomitant formation of TyllA product **27**. However, we also observed formation of a new peak at 11.4 min. Incubation of the reaction mixture for 32 h led to 34% conversion of the starting material to this new product (Figure 5, trace f). On the basis of the dependence of product formation on the presence of TyLB, this compound is likely to be CDP-3-amino-3,6-dideoxy-D-glucose (**28**). High-resolution ESI-MS data of this product purified by HPLC are consistent with the assigned structure (**28**). These results strongly suggest that TyLB is capable of converting **27** to **28**.

DISCUSSION

At the time when the function of FdtA from *A. thermoaerophilus* was first verified, fewer than 10 ORFs encoding homologous proteins had been identified. There are currently at least 65 ORFs exhibiting homology to *fdtA* in the NCBI database, the vast majority of which were uncovered as part of whole genome sequencing projects. These ORFs exist exclusively in bacteria and are often clustered with genes proposed to be involved in outer membrane polysaccharide biosynthesis. A significant portion (18%) of these homologues are found to encode the C-terminal domains of putative bifunctional sugar ketoisomerase/*N*-acetyltransferases. One example of this type of bifunctional enzyme, WxcM from *Xanthomonas campestris* pv. *campestris*, has been shown through genetic studies to be involved in lipopolysaccharide (LPS) biosynthesis (34). Interestingly, *tyllA* and the Spi seq 25 gene from the spiramycin biosynthetic cluster of *Streptomyces ambofaciens* are the only two homologues found in natural product biosynthetic gene clusters. The structure of spiramycin and the organization of its biosynthetic cluster bear significant similarity to those of tylosin. Since a mycamino moiety is also present in the structure of spiramycin, the protein encoded by Spi seq 25 likely serves a role analogous to that of TyllA in mycamino formation in *S. ambofaciens*. It is worth noting that most *fdtA/tyllA* homologues are found in the proximity of genes encoding sugar aminotransferases, with the two often being cotranscribed. In view of the instability of the TyllA product, this close linkage between 3,4-ketoisomerase and aminotransferase may be advantageous, allowing coordinate expression of these two genes in minimizing degradation of the unstable 3-keto sugar product.

The mechanism for the 3,4-ketoisomerization catalyzed by both TyllA and FdtA could proceed with deprotonation at C-3 of **6** to form an enediol (or enediolate) intermediate (i.e., **20** in Scheme 3) followed by reprotonation at C-4 to give the 3-keto product (**7** or **18**). Protein fold and structure analysis of TyllA and FdtA using the Phyre program predicts

Scheme 6: Formation of TDP-1-Eremosamine (**29**) by Route A and an Alternative Route to 3-Amino-2,3,6-trideoxysugars via Route B (**21** → **22** → **23** → **25**)



that these ketoisomerases belong to the RmlC-like cupin superfamily (35). Interestingly, RmlC, the TDP-4-keto-6-deoxy-D-glucose-3,5-epimerase involved in L-rhamnose biosynthesis, is a dimeric protein which also processes **6**. In fact, many members of this superfamily are NDP-4-keto-hexose epimerases responsible for inversion of the C-3 and/or C-5 centers of their substrates. The epimerization catalyzed by these enzymes is thought to involve two sequential cycles of abstraction of the proton α to the keto group followed by reprotonation at the opposite face of the enolate intermediate (36). Thus, there are apparent parallels between the mechanism of RmlC and that proposed for Tyl1a. It is also interesting to note that Tyl1a and FdtA use the same substrate, TDP-4-keto-6-deoxy-D-glucose (**6**), yet form products **7** and **18** (Scheme 1), respectively, which are C-4 epimers of each other. This observation suggests that deoxysugar products with opposite C-4 stereochemistry can be produced by replacing Tyl1a with FdtA (or vice versa). Mechanistically, the stereospecificity of Tyl1a- and FdtA-catalyzed reactions may be determined by the position of the proton-donating residue in the active site relative to C-4 of the sugar substrate. Further studies are required to examine the predicted mechanistic and structural similarities between Tyl1a and RmlC-like epimerases and to decipher the molecular basis for the difference in stereospecificity of Tyl1a- and FdtA-catalyzed reactions.

The identification and in vitro characterization of Tyl1a and the successful reconstitution of the reactions by Tyl1a and TylB to convert **6** to **8** make possible the enzymatic preparation of TDP-3-amino-3,6-dideoxyhexoses, such as **8** and TDP-D-mycaminose (**9**). These sugars can be used in enzymatic synthesis of glycosylated natural products. The presence of 3-amino-2,3,6-trideoxyhexoses in a number of bioactive natural products prompted us to investigate the ability of Tyl1a and TylB to process 2-deoxysugar substrates. The only example of an NDP-3-amino-2,3,6-trideoxyhexose whose biosynthesis has been fully characterized is L-eremosamine (**29**) from the chloroeremomycin pathway of *Amycolatopsis orientalis* (37). This pathway contains a specific aminotransferase, EvaB, capable of acting on C-3 of the highly unstable intermediate TDP-3,4-diketo-2,6-dideoxy-D-glucose (**21**) to give TDP-3-amino-4-keto-2,3,6-trideoxy-D-glucose (**30**), which may serve as a general precursor for 3-amino-2,3,6-trideoxyhexoses (Scheme 6, route A). In the case of L-eremosamine (**29**), compound **30** is further modified by a methyltransferase and an epimerase before reduction of the C-4 keto group.

Having verified the function of Tyl1a, we envisioned that a pathway including a 3,4-ketoisomerization step may be an

alternative biosynthetic route to 3-amino-2,3,6-trideoxyhexoses. This pathway, starting from **6**, involves C-2 deoxygenation and subsequent C-3 ketoreduction to give **22**, followed by 3,4-ketoisomerization and C-3 transamination catalyzed by homologues of Tyl1a and TylB, respectively, to give **25** (Scheme 6, route B). The feasibility of such a pathway could be determined by examining the ability of Tyl1a and TylB to act on 2-deoxysugar substrates. The fact that we were able to demonstrate the formation of **25** enzymatically from **6** via a **6** → **21** → **22** → **23** → **25** route in vitro suggests that this pathway is plausible. However, due to the instability of 3-keto-2,6-dideoxysugar **23**, an excess of TylB relative to Tyl1a is required to yield appreciable amounts of **25**. Since each gene cluster encoding production of 3-amino-2,3,6-trideoxyhexoses discovered thus far possesses an aminotransferase gene closely related to that encoding EvaB, it seems that nature has adopted a more efficient route to make 3-amino-2,3,6-trideoxyhexoses by evolving an aminotransferase that captures the unstable intermediate **21** (route A) rather than one that captures **23** (route B).

While most deoxysugars used in the biosynthesis of secondary metabolites are TDP derivatives, deoxysugar structures bearing CDP, GDP, and UDP groups are not uncommon. Although some studies have demonstrated the ability of the sugar thymidyltransferase RmlA (E_p) from *Sa. enterica* to use UTP (38), there are few studies that have assessed the ability of deoxysugar biosynthetic enzymes to use substrates with alternate nucleotides. Identification of deoxysugar biosynthetic enzymes having relaxed specificity with respect to the nucleoside portion of their NDP-sugar substrates would be useful for preparing NDP-activated sugars. Here, we demonstrated that Tyl1a is capable of turnover of **26**, the CDP version of its natural substrate, but at a significantly reduced rate (~ 400 -fold slower than **6**), requiring high concentrations of the enzyme for significant product formation. However, large amounts of Tyl1a can be readily obtained so that in vitro synthesis of CDP-sugars involving a 3,4-ketoisomerization reaction in their biosynthesis may be feasible using Tyl1a. More extensive testing of deoxysugar biosynthetic enzymes for NDP promiscuity will be necessary to assess the synthetic feasibility of this approach. As the number of X-ray crystal structures of deoxysugar biosynthetic enzymes increases, more sophisticated approaches involving mutagenesis may be employed to generate NDP-promiscuous enzymes for use in construction of a variety of NDP-activated deoxysugars.

The work described herein has established the function of Tyl1a as the TDP-4-keto-6-deoxy-D-glucose-3,4-ketoi-

somerase in the mycaminose biosynthetic pathway in *S. fradiae*. TyllA is only the second example of an enzyme from this newly discovered class to be characterized in vitro. The biochemical characterization of TyllA has significant implications for the correct functional assignment of its many uncharacterized homologues and for the future investigation of the structure and mechanism of this group of enzymes. The availability of TyllA and its demonstrated substrate flexibility are also important for the in vitro and in vivo preparation of a variety of NDP-deoxysugars and, thus, the glycodiversification of natural products.

ACKNOWLEDGMENT

We thank Dr. Eugene Seno at Eli Lilly Research Laboratories for providing us with pSET552, from which TyllA and TyIB were amplified. We also thank Steve Sorey at the NMR Core Facility in the Department of Chemistry and Biochemistry at The University of Texas for his help and expertise in conducting the in situ ^1H NMR assays of TyllA and Dr. Mehdi Moini and co-workers at the Mass Spectrometry Core Facility in the Department of Chemistry and Biochemistry at the University of Texas for mass analysis of samples.

REFERENCES

- Johnson, D. A., and Liu, H.-w. (1999) Deoxysugars: Occurrence, genetics, and mechanisms of biosynthesis, in *Comprehensive Natural Products Chemistry* (Barton, D. H. R., and Nakanishi, K., Eds.) Vol. 3, pp 311–365, Elsevier, Amsterdam.
- Kren, V., and Martinkova, L. (2001) Glycosides in medicine: "The role of glycosidic residue in biological activity", *Curr. Med. Chem.* 8, 1303–1328.
- Weymouth-Wilson, A. C. (1997) The role of carbohydrates in biologically active natural products, *Nat. Prod. Rep.* 14, 99–110.
- Hermann, T. (2005) Drugs targeting the ribosome, *Curr. Opin. Struct. Biol.* 15, 355–366.
- Trefzer, A., Salas, J. A., and Bechthold, A. (1999) Genes and enzymes involved in deoxysugar biosynthesis in bacteria, *Nat. Prod. Rep.* 16, 283–299.
- He, X., and Liu, H.-w. (2002) Formation of unusual sugars: Mechanistic and biosynthetic applications, *Annu. Rev. Biochem.* 71, 701–754.
- Szu, P.-h., He, X., Zhao, L., and Liu, H.-w. (2005) Biosynthesis of TDP-D-desosamine: Identification of a strategy for C4 deoxygenation, *Angew. Chem.* 44, 6742–6746.
- Melançon, C. E. I., Yu, W.-l., and Liu, H.-w. (2005) TDP-mycaminose biosynthetic pathway revised and conversion of desosamine pathway to mycaminose pathway with one gene, *J. Am. Chem. Soc.* 127, 12240–12241.
- Takahashi, H., Liu, Y.-n., and Liu, H.-w. (2006) A two-stage one-pot enzymatic synthesis of TDP-L-mycarose from thymidine and glucose-1-phosphate, *J. Am. Chem. Soc.* 128, 1432–1433.
- Zhao, Z., Hong, L., and Liu, H.-w. (2005) Characterization of the protein encoded by spnR from the spinosyn gene cluster of *Saccharopolyspora spinosa*: Mechanistic implications for forosamine biosynthesis, *J. Am. Chem. Soc.* 127, 7692–7693.
- Blanchard, S., and Thorson, J. S. (2006) Enzymatic tools for engineering natural product glycosylation, *Curr. Opin. Chem. Biol.* 10, 263–271.
- Salas, J. A., and Mendez, C. (2005) Biosynthesis pathways for deoxysugars in antibiotic-producing Actinomycetes: Isolation, characterization and generation of novel glycosylated derivatives, *J. Mol. Microbiol. Biotechnol.* 9, 77–85.
- Hong, J. S. J., Park, S. H., Choi, C. Y., Sohng, J. K., and Yoon, Y. J. (2004) New oliviosyl derivatives of methymycin/pikromycin from an engineered strain of *Streptomyces venezuelae*, *FEMS Microbiol. Lett.* 238, 391–399.
- Bryskier, A. J. (1993) in *Macrolides: Chemistry, pharmacology, and clinical uses* (Bryskier, A. J., Butzler, J.-P., Neu, H. C., and Tulkens, P. M., Eds.) Arnette Blackwell, Paris.
- Baltz, R. H., and Seno, E. T. (1988) Genetics of *Streptomyces fradiae* and tylosin biosynthesis, *Annu. Rev. Microbiol.* 42, 547–574.
- Chen, H., Guo, Z., and Liu, H.-w. (1998) Expression, purification, and characterization of TyIM1, an *N,N*-dimethyltransferase involved in the biosynthesis of mycaminose, *J. Am. Chem. Soc.* 120, 9951–9952.
- Cundliffe, E., Bate, N., Butler, A., Fish, S., Gandeche, A., and Merson-Davies, L. (2001) The tylosin biosynthetic genes of *Streptomyces fradiae*, *Antonie van Leeuwenhoek* 79, 229–234.
- Chen, H., Yeung, S.-M., Que, N. L. S., Muller, T., Schmidt, R. R., and Liu, H.-w. (1999) Expression, purification, and characterization of TyIB, an aminotransferase involved in the biosynthesis of mycaminose, *J. Am. Chem. Soc.* 121, 7166–7167.
- Naudorf, A., and Klaffke, W. (1996) Substrate specificity of native dTDP-D-glucose-4,6-dehydratase: Chemo-enzymic syntheses of artificial and naturally occurring deoxy sugars, *Carbohydr. Res.* 285, 141–150.
- Stein, A., Kula, M.-R., Elling, L., Versack, S., and Klaffke, W. (1995) Synthesis of dTDP-6-deoxy-4-ketoglucose and analogs with native and recombinant dTDP-glucose-4,6-dehydratase, *Angew. Chem.* 34, 1748–1749.
- Borisova, S. A., Zhao, L., Sherman, D. H., and Liu, H.-w. (1999) Biosynthesis of desoamine: Construction of a new macrolide carrying a genetically designed sugar moiety, *Org. Lett.* 1, 133–136.
- Pfoestl, A., Hofinger, A., Kosma, P., and Messner, P. (2003) Biosynthesis of dTDP-3-acetamido-3, 6-dideoxy- α -D-galactose in *Aneurinibacillus thermoaerophilus* L420-91^T, *J. Biol. Chem.* 278, 26410–26417.
- Bradford, M. M. (1976) A rapid and sensitive method for the quantitation of microgram quantities of protein utilizing the principle of protein-dye binding, *Anal. Biochem.* 72, 248–254.
- Laemmli, U. K. (1970) Cleavage of structural proteins during the assembly of the head of bacteriophage T4, *Nature* 227, 680–685.
- Andrews, P. (1964) Estimation of the molecular weights of proteins by Sephadex gel-filtration, *Biochem. J.* 91, 222–233.
- Sambrook, J., and Russell, D. W. (2001) *Molecular cloning: A laboratory manual*, 3rd ed., Cold Spring Harbor Laboratory Press, Plainview, NY.
- Chen, H., Agnihotri, G., Guo, Z., Que, N. L. S., Chen, X. H., and Liu, H.-w. (1999) Biosynthesis of mycarose: Isolation and characterization of enzymes involved in the C-2 deoxygenation, *J. Am. Chem. Soc.* 121, 8124–8125.
- Waldron, C., Matsushima, P., Rosteck, P. R., Jr., Broughton, M. C., Turner, J., Madduri, K., Crawford, K. P., Merlo, D. J., and Baltz, R. H. (2001) Cloning and analysis of the spinosad biosynthetic gene cluster of *Saccharopolyspora spinosa*, *Chem. Biol.* 8, 487–499.
- Draeger, G., Park, S.-H., and Floss, H. G. (1999) Mechanism of the 2-deoxygenation step in the biosynthesis of the deoxyhexose moieties of the antibiotics granatacin and oleandomycin, *J. Am. Chem. Soc.* 121, 2611–2612.
- Chen, X. M. H., Ploux, O., and Liu, H.-w. (1996) Biosynthesis of 3,6-dideoxyhexoses: In vivo and in vitro evidence for protein-protein interaction between CDP-6-deoxy-L-threo-D-glycero-4-hexulose-3-dehydratase (E1) and its reductase (E3), *Biochemistry* 35, 16412–16420.
- Thorson, J. S., Lo, S. F., Ploux, O., He, X., and Liu, H.-w. (1994) Studies of the biosynthesis of 3,6-dideoxyhexoses: Molecular cloning and characterization of the asc (ascarylose) region from *Yersinia pseudotuberculosis* serogroup VA, *J. Bacteriol.* 176, 5483–5493.
- Thorson, J. S., Kelly, T. M., and Liu, H.-w. (1994) Cloning, sequencing, and overexpression in *Escherichia coli* of the α -D-glucose-1-phosphate cytidylyltransferase gene isolated from *Yersinia pseudotuberculosis*, *J. Bacteriol.* 176, 1840–1849.
- Merson-Davies, L. A., and Cundliffe, E. (1994) Analysis of five tylosin biosynthetic genes from the *tylIBA* region of the *Streptomyces fradiae* genome, *Mol. Microbiol.* 13, 349–355.
- Vorholter, F.-J., Niehaus, K., and Puhler, A. (2000) Lipopolysaccharide biosynthesis in *Xanthomonas campestris* pv. *campestris*: A cluster of 15 genes is involved in the biosynthesis of the LPS O-antigen and the LPS core, *Mol. Genet. Genomics* 266, 79–95.

35. Dunwell, J. M., Culham, A., Carter, C. E., Sosa-Aguirre, C. R., and Goodenough, P. W. (2001) Evolution of functional diversity in the cupin superfamily, *Trends Biochem. Sci.* 26, 740–746.
36. Jakimowicz, P., Tello, M., Freel, Meyers, C. L., Walsh, C. T., Buttner, M. J., Field, R. A., and Lawson, D. M. (2006) The 1.6-Å resolution crystal structure of NovW: A 4-keto-6-deoxy sugar epimerase from the novobiocin biosynthetic gene cluster of *Streptomyces spheroides*, *Proteins: Struct., Funct., Bioinf.* 63, 261–265.
37. Chen, H., Thomas, M. G., Hubbard, B. K., Losey, H. C., Walsh, C. T., and Burkart, M. G. (2000) Deoxysugars in glycopeptide antibiotics: Enzymatic synthesis of TDP-L-epivancosmaine in chloroeremomycin biosynthesis, *Proc. Natl. Acad. Sci. U.S.A.* 97, 11942–11947.
38. Jiang, J., Biggins, J. B., and Thorson, J. S. (2000) A general enzymatic method for the synthesis of natural and “unnatural” UDP- and TDP-nucleotide sugars, *J. Am. Chem. Soc.* 122, 6803–6804.

BI061907Y